

Identifying and quantifying mechanisms responsible for the substantial loss of HHFW power in the SOL of NSTX

R.J. Perkins¹, J.-W. Ahn², R. E. Bell¹, N. Bertelli¹, A. Diallo¹, S. Gerhardt¹, T. K. Gray², D. L. Green², E. F. Jaeger², J. C. Hosea¹, M. A. Jaworski¹, B. P. LeBlanc¹, G. J. Kramer¹, A. McLean², R. Maingi¹, C. K. Phillips¹, L. Roquemore¹, P. M. Ryan², S. Sabbagh³, G. Taylor¹, J. R. Wilson¹

¹PPPL, Princeton University, Princeton, NJ 08540, USA

²ORNL, Oak Ridge, TN 37831, USA

³Columbia University, New York, NY 10027, USA

NSTX can exhibit a major loss of high-harmonic fast wave (HHFW) power to the upper and lower divertor regions along scrape-off layer (SOL) field lines passing in front of the antenna [1-6], creating bright spirals on the upper and lower divertor regions (Fig. 1). The losses can be up to 60% of the HHFW power, while the heat flux in the observed RF spirals can be up to 2 MW/m² for 2 MW of applied HHFW power [2,4]. Recent simulations using the full-wave code AORSA [7] have verified that the RF fields in the SOL become significant as the right-hand cutoff for fast waves is moved toward and beyond the antenna [8]. However, the underlying mechanism(s) by which these fields produce a heat flux on the divertor has not yet been identified, which limits our understanding of how these losses scale and how they might be mitigated. Possible candidates for the loss mechanism(s) are: (1) a two-stream instability of the RF currents that volumetrically heats the SOL plasma [9], which in turn flows to the divertor along field lines; (2) far-field RF sheaths at the divertor that drive ion bombardment into the divertor [10]; and (3) parametric decay instability of the HHFW wave into an ion Bernstein wave that damps on ions at appropriate ion-cyclotron layers [11]. Here we investigate the possible contributions of each candidate mechanism and compare them to experimental data in an effort to confirm one or more candidates. This work will guide future experimentation on NSTX-U and other machines in definitely identifying the mechanisms and minimizing their effects, which is important for optimizing high-power long-pulse ICRF heating on ITER while guarding against excessive erosion in the divertor region.

The heat flux produced by each candidate mechanism scales differently with input HHFW power, and these expected scalings can be compared, to the extent possible, against the estimated

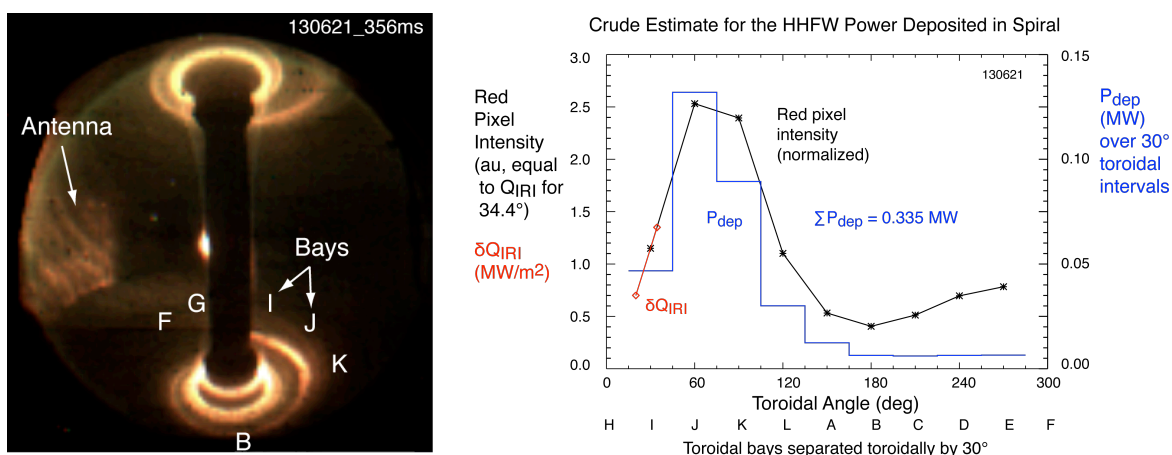


FIGURE 1. LEFT: Visible-light image of the spirals on the upper and lower divertor for an ELM-free H-mode plasma with $P_{RF} = 1.8$ MW, -90° phasing, $P_{NB} = 2$ MW, $I_p = 1$ MA, $B_T = 0.55$ T. RIGHT: A crude estimate of the RF power deposited in the spiral. The toroidal variation of the red pixel intensity (black curve) serves as a proxy for the variation of the heat flux intensity, which is only measured at Bay I. The black curve is normalized so that two measurements of Q_{IRI} , the RF-produced heat flux at two toroidal positions near Bay I, lie on it. The blue curve is then an estimate of the power deposited in each section of the spiral. The total power deposited from Bay I to Bay E is estimated to be around 0.335 MW. Q_{IRI} is obtained by subtracting data taken at 0.357 s (during the RF pulse) with data from 0.257 s (at start of the RF pulse).

experimental scaling on NSTX. While the total RF-produced heat flux to the divertor cannot be accurately determined without more complete infrared (IR) camera coverage, a rough estimate has been obtained in Fig. 1 [12]. The likelihood of each mechanism will be constrained by analyzing the scaling of such estimates of the RF-produced heat flux against the applied HHFW power. Additionally, we will analyze the change in Langmuir probe characteristics when that probe lies under the RF spiral relative to those for nearby probes that do not. For instance, for the case in Fig. 2, we assume the change is entirely due to a shift in floating potential, which then specifies an RF sheath voltage peak amplitude of ~ 76 V from the relation $\exp(\Delta_i/T_e) = I_0(V_{RF}/T_e)$ [13].

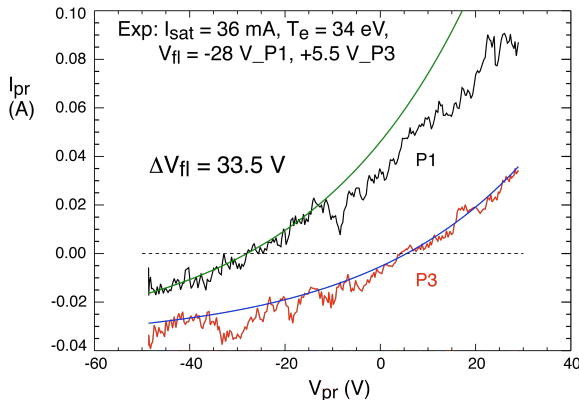


Figure 2. Shift in floating potential under the lower divertor RF spiral. Characteristics are averaged over 6×1 ms sweeps starting at 0.362 s during the RF pulse. Probe 1 is at $R = 63.8$ cm under the spiral and P3 is at $R = 67.5$ cm away from the spiral. $\Delta V_{fl} \approx 33.5$ V and $T_e \approx 34$ eV equates to $V_{RF\ peak} \approx 76$ V. ($B_T = 5.5$ kG, $I_p = 0.65$ MA, $P_{RF} = 1.1$ MW from $t = 0.2$ s - .41 s, helium.)

We also constrain the candidate mechanisms by using the numerically-computed RF fields to estimate the losses and comparing these to the experimentally observed heat flux. The RF fields will be taken from AORSA and also from a cylindrical cold-plasma model. The latter models the core as a high-density plasma cylinder and the SOL as a lower-density annulus; the simplified geometry will aid in interpreting the field structures given by AORSA. Fields from both codes can be used to compute the RF currents in the plasma for comparison to the two-stream instability threshold, and the fields from AORSA at the divertor can be used to estimate the amplitude at the RF sheath.

Direct measurements of RF fields and heat deposition in NSTX-U will ultimately be used to ascertain the importance and magnitude of each of the proposed loss mechanisms. Prior to that, this work will constrain the possible mechanisms and provide guidance in designing such experiments. The field-aligned RF losses studied here could impact other fusion devices, including ITER, as the recent results from AORSA [8] suggest that the enhanced RF fields in the SOL are a property of fast waves in general.

This work was supported by DOE Contract No. DE-AC02-09CH11466.

- [1] J.C. Hosea *et al.*, *Phys. Plasmas* **15** (2008) 056104.
- [2] J.C. Hosea *et al.*, *AIP Conf. Proc.* **1187** (2009) 105.
- [3] C.K. Phillips *et al.*, *Nucl. Fusion* **49** (2009) 075015.
- [4] G. Taylor *et al.*, *Phys. Plasmas* **17** (2010) 056114.
- [5] R. J. Perkins *et al.*, *Phys. Rev. Lett.* **109**, (2012) 045001.
- [6] R. J. Perkins *et al.*, *Nucl. Fusion* **53**, (2013) 083025.
- [7] D.L. Green *et al.*, *Phys. Rev. Lett.* **107** (2011) 145001.
- [8] N. Bertelli *et al.*, submitted to *Nucl. Fusion* (2014)
- [9] J.C. Hosea, "UHF-plasma interaction: the two-stream instability of a current carrying plasma", Ph.D. dissertation (1966).
- [10] D. A. D'Ippolito *et al.*, *Phys. Plasmas*, **15** (2008) 102501.
- [11] J. R. Wilson *et al.*, *AIP Conf. Proc.* **787** (2005) 66.
- [12] R. J. Perkins *et al.*, to appear in *AIP Conf. Proc.*
- [13] A. Boschi and F. Magistrelli, *Nuovo Cimento* **29** (1963) 487.